Advanced finite-difference methods for seismic modeling

Yang Liu[1,2] and Mrinal K Sen[2]

[1]State Key Laboratory of Petroleum Resource and Prospecting (China University of Petroleum, Beijing), Beijing, 102249, China

[2]The Institute for Geophysics, John A. and Katherine G. Jackson School of Geosciences, The University of Texas at Austin, 10100 Burnet Road, R2200 Austin, TX 78758, USA

E-mail: wliuyang@vip.sina.com, mrinal@ig.utexas.edu

Abstract

The finite-difference methods (FDMs) have been widely used in seismic modeling and migration. In this paper, we review the conventional arbitrary-order explicit FDMs and their recent developments, including arbitrary even-order implicit FDMs for standard grids and arbitrary even-order time-space domain FDMs for acoustic wave equations. For a given accuracy, an arbitrary even-order FDM can provide a trade-off between the order number and grid size. These explicit FDMs are the most popular in seismic modeling community. The finite-difference methods that are implicit in space are not very common because they generally require more computer resources than the explicit FDMs. Here we show that a new class of implicit FDMs can be derived that require solving a tri-diagonal system, which makes the resulting algorithm computationally very efficient. Therefore, some high-order explicit FDM may be replaced by an implicit FDM of some order to decrease the computation time without affecting the accuracy. We further demonstrate that we can also derive the FD coefficients in the joint time-space domain. These high-order spatial finite-difference stencils designed in joint time-space domain, when used in acoustic wave equation modeling, can provide even greater accuracy than those designed in the space domain alone under the same discretization. We demonstrate performance of these algorithms using some realistic 2D numerical examples.

Introduction

The finite-difference method (FDM), one of the most popular methods of numerical solution of partial differential equations, has been widely used in seismic modeling (e.g., Kelly et. al., 1976; Virieux, 1986; Igel et. al. 1995; Etgen, 2007; Bansal and Sen, 2008) and migration (Claerbout, 1985; Li, 1991; Zhang et. al., 2000; Fei et. al. 2008). The development of an FD operator is based generally on a Taylor series representation of a function (the wavefield) resulting in a formulation for numerical evaluation of the derivatives appearing in the wave equation. The accuracy of these operators is dependent on the order of approximation, namely, the number of terms used in the Taylor series representation of the function. Thus a discrete version of the wave equation is derived where the wavefield is propagated starting from the source location (the initial condition). In general, accuracy of the derivative calculation for a given order depends on grid spacing. A small grid size helps to increase the accuracy but results in a large number of grids to represent a geologic model. Thus, there is a substantial increase in memory and floating point operations making these methods prohibitive for realistic modeling of complex geological structures in the seismic frequency range.

To improve the accuracy and stability of a FDM in numerical modeling, many methods have been developed including difference schemes of variable grid (Wang et. al., 1996; Hayashi et. al., 1999), irregular grid (Opršal et. al., 1999), standard staggered grid (Virieux, 1986; Levander, 1988; Robertsson et al., 1994; Graves, 1996), rotated staggered grid (Gold et al., 1997; Saenger et. al., 2004; Bohlen et. al., 2006), variable time step (Tessmer, 2000) and implicit methods (Emerman et al, 1982; Zhang and Zhang, 2007).

One obvious approach to improve on the accuracy of FD calculation is to design high order operators for computing the derivatives (Dablain, 1986; Fornberg, 1987; Crase, 1990; Liu et al, 1998; Dong, 2000; Pei, 2004; Chen, 2007; Liu et al, 2008; Liu and Sen, 2009). In this paper, we review the developments of arbitrary even-order FDMs for seismic modeling, including EFDMs (explicit FDMs), IFDMs (implicit FDMs) and time-space domain FDMs.

First, we briefly review the seismic wave equations, finite difference, dispersion, stability and the necessity of high-order finite differences. We restrict our discussion to acoustic wave equation because of the ease of algebra. These are followed by description of EFDMs, new IFDMs and time-space domain FDMs. Finally, we show some numerical examples to demonstrate the salient features of different algorithms.

Background

Seismic wave equations: finite difference approximations

Seismic wave equations, used to describe seismic wave propagation in the subsurface, are typically partial differential equations containing spatial and temporal derivatives. The constant density acoustic wave equation has been used most widely in seismic modeling, migration and inversion. The 1D acoustic wave equation in a homogenous medium is given by

$$\frac{\partial^2 p}{\partial x^2} = \frac{1}{v^2}\frac{\partial^2 p}{\partial t^2}, \qquad \text{..........(1)}$$

where,

$p = p(x,t)$ is a scalar wave field, and v is the velocity.

From Equation (1), we can see that the wave field is a function of the spatial coordinate and time.

The following 2nd-order finite difference is usually used for calculating temporal derivatives,

$$\frac{\partial^2 p}{\partial t^2} \approx \frac{1}{\tau^2}\left[-2p_{j,m} + \left(p_{j,m-1} + p_{j,m+1}\right)\right], \qquad \text{..........(2)}$$

where,

$$p_{j,m} = p(jh, m\tau), \qquad \text{..........(3)}$$

h and τ are grid size and time step respectively (see Figure 1). For the 2nd-order continuous-time wave field,

$$\frac{\partial^2 p}{\partial t^2} = \lim_{\tau \to 0}\frac{1}{\tau^2}\left[-2p_{j,m} + \left(p_{j,m-1} + p_{j,m+1}\right)\right]. \qquad \text{..........(4)}$$

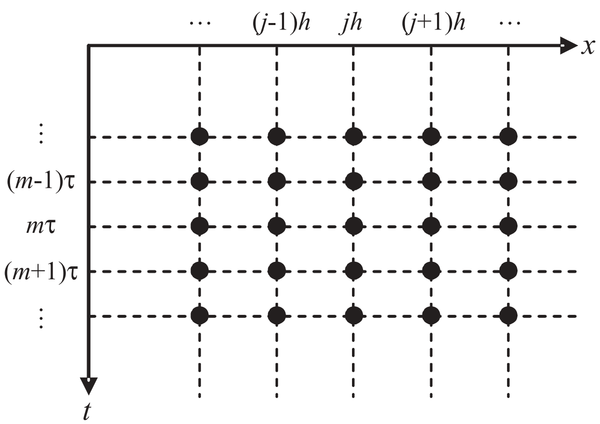

Fig.1 Illustration of grids for wave fields in the time-space domain

Thus, a smaller time step leads to greater accuracy for computing temporal derivatives. Higher order approximation of Equation (2) can also be derived from the Taylor series.
Note that Equation (2) requires the wavefield values at the current time step, past time step and a future time step at a given spatial point. Such a scheme is called an explicit scheme in time. Generally, an explicit high-order finite difference on the temporal derivatives requires large computer memory and is usually unstable. An equation similar to Equation (2) can also be derived for a spatial derivative which will require the wavefield values at the current grid and its two neighboring grids, at a given time step. Such a scheme is called an explicit scheme in space. However, unlike the temporal derivatives, a high-order finite difference on the spatial derivatives is stable. A (2N)th-order finite difference formula for the 2nd-order spatial derivative is given by

$$\frac{\partial^2 p}{\partial x^2} \approx \frac{1}{h^2}\left[c_0 p_{j,m} + \sum_{n=1}^{N} c_n\left(p_{j-n,m} + p_{j+n,m}\right)\right], \qquad \text{..........(5)}$$

where, c_n are the finite-difference coefficients and their expressions are given in the following section. When $N = 1$, we can obtain $c_0 = -2$, $c_1 = 1$, then Equation (5) is similar to Equation (2). When $N = 2$, then $c_0 = -5/2$, $c_1 = 4/3$, $c_2 = -1/12$. Also, a smaller grid size can help attain greater accuracy for spatial derivatives.

Substituting Equations (2) and (5) into Equation (1), we have

$$\frac{1}{h^2}\left[c_0 p_{j,m} + \sum_{n=1}^{N} c_n\left(p_{j-n,m} + p_{j+n,m}\right)\right] \approx \frac{1}{v^2\tau^2}\left[-2p_{j,m} + \left(p_{j,m-1} + p_{j,m+1}\right)\right]. \qquad \text{..........(6)}$$

Rearranging Equation (6), we obtain,

$$p_{j,m+1} = 2p_{j,m} - p_{j,m-1} + r^2\left[c_0 p_{j,m} + \sum_{n=1}^{N} c_n\left(p_{j-n,m} + p_{j+n,m}\right)\right], \qquad \text{..........(7)}$$

where, $r = v\tau/h$. Equation (7) is the recursion formula for solving 1D wave equation by a finite-difference method. The recursion begins with the wave field values known at two successive time steps $t=0$ and $t=\tau$. The wavefield values at a future time step at all the spatial locations are computed using Equation (7).

Dispersion

One obvious observation we can make is that truncation of terms in a Taylor series expansion causes inaccuracies in the evaluation of a derivative. It also causes frequency-dependent numerical errors due to truncation of higher order terms, even when the material properties are not frequency dependent. In fact, we observe a numerical phenomenon called 'dispersion' that is similar to what is observed in dissipative or attenuating media in which propagation velocities are frequency-dependent. Frequency-dependent numerical dispersion is observed even in non-attenuating media due to inadequate sampling of wavefields in space and time.

Here, we discuss the dispersion generated by the recursion formula (7). Using a plane wave theory, we let

$$p_{j,m} = e^{\mathrm{i}(kx-\omega t)} = e^{\mathrm{i}(jkh-m\omega\tau)}, \qquad \text{..........(8)}$$

where, k is the wavenumber, ω is the angular frequency, and $\mathrm{i}=\sqrt{-1}$. Substituting Equation (8) into (7) and simplifying it, we have

$$r^2\left[c_0 + 2\sum_{n=1}^{N} c_n \cos(nkh)\right] = 2\left[\cos(\omega\tau)-1\right], \qquad \text{..........(9)}$$

which can be solved for a frequency ω; a group velocity is given by the ratio of frequency ω to wavenumber k. The group or dispersion velocity is

$$v_{\mathrm{FD}} = \frac{\omega}{k} = \frac{1}{k\tau}\cos^{-1}\left[\frac{r^2}{2}\left(c_0 + 2\sum_{n=1}^{N} c_n \cos(nkh)\right)\right]. \qquad \text{..........(10)}$$

Note that, v_{FD} is the velocity with which the wave propagates through numerical grids. This expression shows that the dispersion velocity depends on the medium velocity v, grid size h, time step τ, wavenumber k and finite-different coefficients c_n.

Using Equation (10) and $r = v\tau/h$, we define a parameter δ to describe the dispersion

$$\delta = \frac{v_{\mathrm{FD}}}{v} = \frac{1}{rkh}\cos^{-1}\left[\frac{r^2}{2}\left(c_0 + 2\sum_{n=1}^{N} c_n \cos(nkh)\right)\right] \text{..........(11)}$$

Note that the parameter δ is the ratio of dispersion velocity to the true velocity of the medium and in fact it is a measure of numerical error of finite difference approximation. If δ equals 1, there is no dispersion. If δ is far from 1, a large dispersion will occur. Thus our primary goal is to make δ close to 1 by a proper choice of grid spacing h for a given velocity and frequency. Since kh is equal to π at the Nyquist frequency, kh only ranges from 0 to π when calculating δ.

Here, we show a 1D modeling example to examine this effect. Modeling parameters are shown in Figure 2. Initial conditions for the modeling are

$$p(x,t)\big|_{t=0} = (x-x_0)e^{-\frac{\alpha^2}{4h^2}(x-x_0)^2}, \qquad \text{..........(12a)}$$

$$\left.\frac{\partial p(x,t)}{\partial t}\right|_{t=0} = 0, \qquad \text{..........(12b)}$$

where x_0 is the location of the center of the source, and α^2 is an attenuation coefficient. Figures 2(a) and 2(b) show exact and modeling results with snapshots. In this 1D case, it can be seen from the snapshots that high-wavenumber components propagate with lower velocity. Figure 2(c) shows the dispersion curve of this finite-difference modeling. It follows that high-wavenumber components have lower than the true velocity. This is well demonstrated with Figure 2(b). In Figure 2(b), because of their different velocities, different-wavenumber components gradually disperse as the wave propagates, which is the so-called dispersion phenomenon.

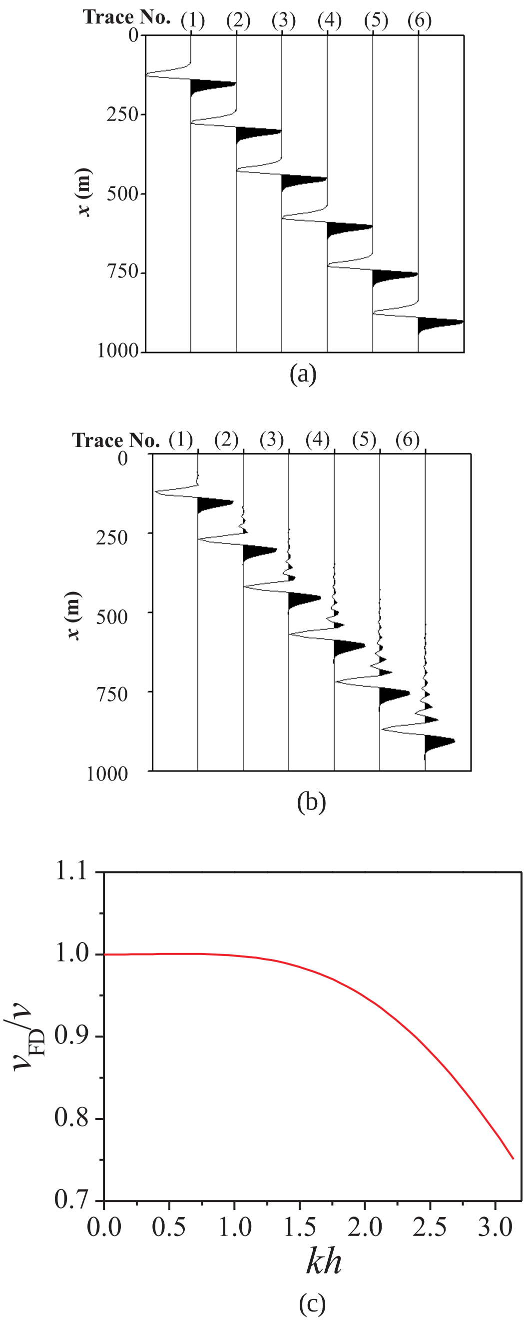

Fig.2 Illustration of dispersion in finite-difference modeling: (a) Snapshots from 1D analytic solution; (b) Snapshots from 1D acoustic wave equation modeling by finite-difference recursion Formula (7), N=2. Snapshots (1) to (6) are recorded at 0.05s, 0.1s, 0.15s, 0.2s, 0.25s and 0.3sm, respectively. (c) The dispersion curve of this finite-difference modeling. The model is homogeneous, v = 3000m/s, model size is 1000m. The modeling parameters are: h = 10m, τ = 0.001s, $\alpha^2 = 1$, $x_0 = 0$.

Stability

Recursion formula, such as the one used in Equation (7), is commonly used to perform finite-difference modeling. If the modeling parameters are inappropriate, for example, if time step is too large, the recursion will be unstable. In other words, the wavefield will grow and will eventually exceed the machine precision.

We will now use a conventional eigenvalue method (Chen and Guan, 1989) of stability analysis to derive the stability condition for recursion formula (7). Let

$$q_{j,m} = p_{j,m-1}, \quad U_{j,m} = \left(p_{j,m}, q_{j,m}\right)^T = \left(w_{1,m}, w_{2,m}\right)^T e^{ijkh} = \boldsymbol{W}_m e^{ijkh}. \qquad \text{..........(13)}$$

According to Equation (7) and (13), we can obtain (see Appendix A)

$$\boldsymbol{W}_{m+1} = \boldsymbol{G}\boldsymbol{W}_m = \begin{bmatrix} g & -1 \\ 1 & 0 \end{bmatrix} \boldsymbol{W}_m, \qquad \text{..........(14)}$$

where **G** is a transition matrix,

$$g = 2 + 2r^2 \sum_{n=1}^{N} c_n \left[\cos(nkh) - 1\right]. \qquad \text{..........(15)}$$

When the absolute values of the transition matrix eigenvalues are less than or equal to 1, the recursion is stable. If $|g| \le 2$, the roots of the eigenvalue equation $\lambda^2 - g\lambda + 1 = 0$ will be less than or equal to 1. Then, the following stability condition can be obtained

$$r \le s = \left(\sum_{n=1}^{N_1} c_{2n-1}\right)^{-1/2}, \qquad \text{..........(16)}$$

where, N_1 =int [$(N+1)/2$] and int is a function to get the integer part of a value. We calculate the variation of s with N, which is shown in Figure 3. From this figure, we can see that the area of r for stable recursion decreases with the increase of N.

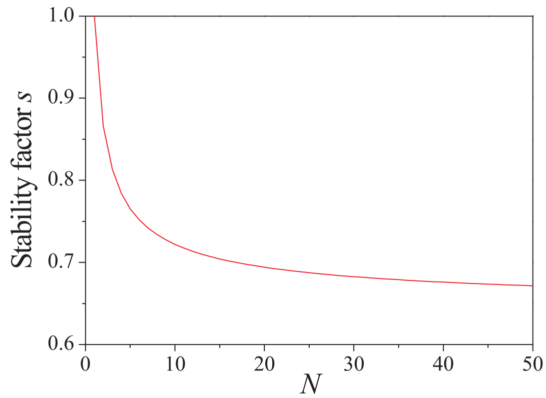

Fig.3 Illustration of stability condition of 1D acoustic wave equation modeling by finite-difference recursion Formula (7). The recursion is stable when $r \le s$.

Necessity of high-order finite differences on the spatial derivatives

In the previous section, we demonstrated the presence of grid dispersion in the acoustic wavefield modeled by a 2nd-order finite-difference operator. There are several ways to reduce the dispersion. The first way is to decrease the grid size. Due to the limitation of computer memory, we cannot use a very small grid size, especially for 3D modeling. The second approach is to decrease the time step. Figure 4(a) shows dispersion curves of low-order finite-difference modeling for different time steps, which suggest that decreasing the time step will decrease the dispersion of low-wavenumber components, but will not decrease the dispersion of middle- and high-wavenumber components. The third approach is to use high-order finite differences. Figure 4(b) shows dispersion curves for high-order finite-difference modeling for different time steps, which suggest that decreasing time step will decrease the dispersion of low- and middle-wavenumber components. Comparing Figure 4(a) with 4(b), we conclude that a high-order finite difference on the spatial derivatives is necessary to reduce dispersion. One other approach to suppress the grid dispersion is to use staggered grids (e.g., Virieux, 1986; Kindelan et al 1990; Graves, 1996; Saenger and Bohlen, 2004; Bohlen and Saenger; 2006). However, in this paper we will discuss standard grids only.

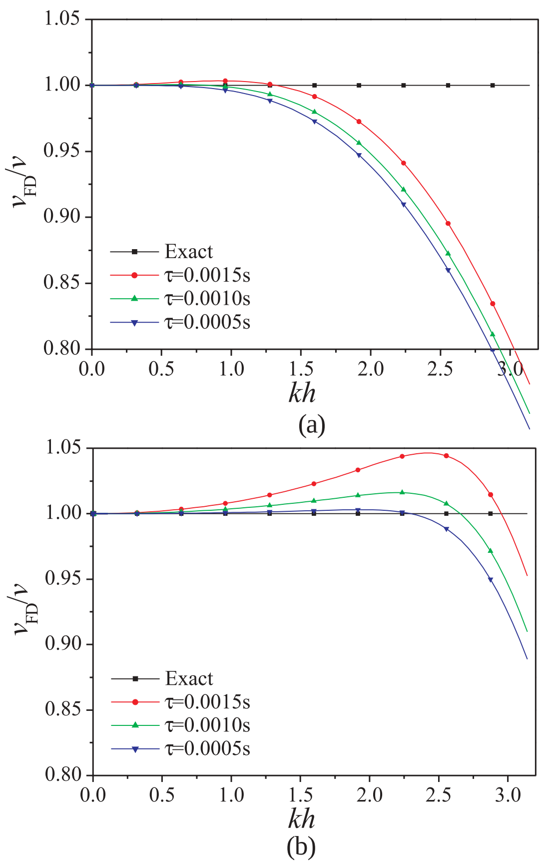

Fig. 4 Dispersion curves for 1D acoustic wave equation modeling by finite-difference recursion Formula (7) for different time steps. v = 3000m/s, h = 10m. (a) Low-order finite difference on spatial derivatives, N=2; (b) High-order finite difference on spatial derivatives, N=10.

Explicit finite-difference methods

Centered finite-difference formulas in a standard grid scheme are usually used to numerically solve partial differential equations, which generally involve the first-order and the second-order derivatives in a seismic modeling application. In the following, we introduce centered finite-difference formulas with arbitrary even-order accuracy for the first-order and the second-order derivatives.

Explicit finite-difference formula for the 1st-order derivatives

A (2*N*)th-order finite-difference formula for the first-order derivatives can be expressed as (Dablain, 1986)

$$\frac{\partial p}{\partial x} \approx \frac{1}{h}\sum_{n=-N}^{N} c_n p(x+nh), \qquad \text{.............(17)}$$

where, $p(x)$ is a function of x, x is a real variable, h is a small constant value of grid size, N is a positive integer; the finite-difference coefficient c_n is an odd discrete sequence. Appendix B gives a methodology based on plane wave theory for deriving finite-difference coefficients. c_n can be computed by the following formula (Fornberg, 1987; Liu et. al., 1998, 2008; Liu and Sen, 2009a)

$$c_n = \frac{(-1)^{n+1}}{2n}\prod_{1\le m\le N, m\ne n}\left|\frac{m^2}{m^2-n^2}\right|, \quad n=1,2,\ldots,N. \qquad \text{........(18)}$$

When $N \to \infty$,

$$c_n = \frac{(-1)^{n+1}}{n} \quad n=1,2,\ldots,\infty. \qquad \text{..........(19)}$$

Thus, there exists a limit at which we can attain infinite accuracy theoretically and at this limit we arrive at the pseudospectral method (Fornberg, 1987).

Explicit finite-difference formula for the 2nd-order derivatives

A (2*N*)th-order finite-difference formula for the second-order derivatives can be expressed as

$$\frac{\partial^2 p}{\partial x^2} \approx \frac{1}{h^2}\sum_{n=-N}^{N} c_n p(x+nh), \qquad \text{..........(20)}$$

where, the difference coefficient, c_n an even discrete sequence, can be computed by the following formulas (Liu et. al., 1998, 2008; Liu and Sen, 2009a)

$$c_n = \begin{cases} \dfrac{(-1)^{n+1}}{n^2}\displaystyle\prod_{1\le m\le N, m\ne n}\left|\frac{m^2}{m^2-n^2}\right| & (n=1,2,\ldots,N) \\ 2\displaystyle\sum_{m=1}^{N} c_m & (n=0). \end{cases} \qquad \text{........(21)}$$

When $N \to \infty$,

$$c_n = \frac{2(-1)^{n+1}}{n^2}, \quad n=(1,2,\ldots,\infty). \qquad \text{...........(22)}$$

To examine the accuracy of these finite-difference formulas (17) and (20), the following expressions are used (Liu and Sen, 2009a)

$$f_1(\alpha) = \sum_{n=1}^{N} c_n \sin(2n\alpha), \qquad \text{...........(23a)}$$

$$f_2(\alpha) = \sqrt{-\frac{1}{4}c_0 - \frac{1}{2}\sum_{n=1}^{N} c_n\cos(2n\alpha)}, \qquad \text{...........(23b)}$$

where, $\alpha = kh/2$, k is wavenumber. When calculating the values of the above expressions, α only ranges from 0 to $\pi/2$ because kh is equal to π at the Nyquist frequency. The calculated values from formulas (23a) and (23b) are compared with the exact values of α for different order numbers determined by N, shown in Figure 5. We notice that the

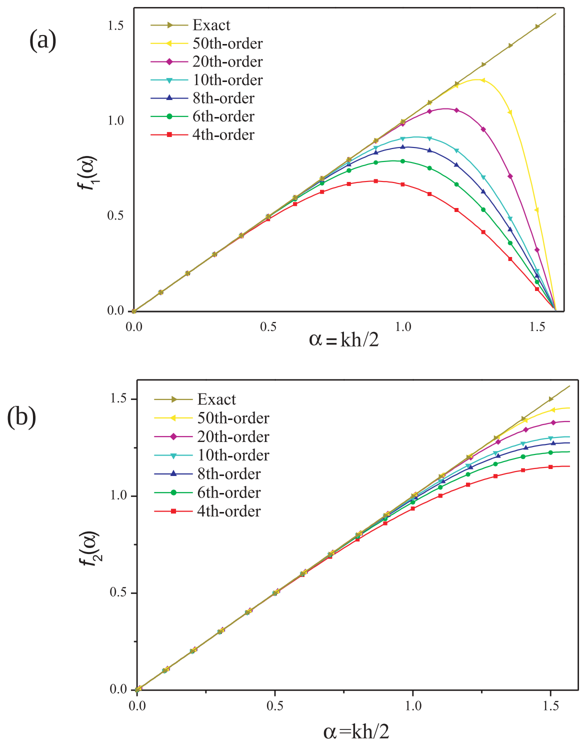

Fig. 5 Accuracy of explicit finite-difference formulas
(a) The exact α and $f_1(\alpha)$ of EFDM with different order numbers for the first-order derivatives
(b) The exact α and $f_2(\alpha)$ of EFDM with different order numbers for the second-order derivatives

accuracy increases with the increase of the order number.

Implicit finite-difference methods

We noted in the previous section that an EFDM directly calculates the derivative value at some point using the function values at that point and at its neighboring points. However, an IFDM (implicit FDM) expresses the derivative value at some point in terms of the function values at that point and at its neighboring points and the derivative values at its neighboring points. For example, a compact finite-difference method (CFDM) is one such IFDM (Lele 1992). However, IFDMs are usually considered expensive due to the requirement of solving a larger number of equations and are therefore not very popular. Liu and Sen (2009a) derived new implicit formulas for space derivatives with arbitrary even-order accuracy for arbitrary-order derivatives. Their approach requires solving tridiagonal matrix equations only. They also showed that a high-order explicit method may be replaced by an implicit method of some order, which will increase the accuracy but not the computational cost.

We first introduce Claerbout's idea (Claerbout 1985) upon which the methods of Liu and Sen (2009a) are developed. The 2nd-order difference operator for a function is expressed as

$$\frac{\partial^2 p}{\partial x^2} \approx \frac{\delta^2 p}{\delta x^2} = \frac{p(x+h)+p(x-h)-2p(x)}{h^2}. \qquad \text{……….(24).}$$

The accuracy of finite difference can be improved by adding higher-order terms, that is,

$$\frac{\partial^2 p}{\partial x^2} \approx \frac{\delta^2 p}{\delta x^2} - b\frac{\delta^4 p}{\delta x^4}, \qquad \text{……….(25).}$$

where b is an adjustable constant. This expression is rarely used – it can be changed to the following form (Claerbout 1985)

$$\frac{\partial^2 p}{\partial x^2} \approx \frac{\dfrac{\delta^2 p}{\delta x^2}}{1+b\dfrac{\delta^2}{\delta x^2}}. \qquad \text{……….(26).}$$

This equation has greater accuracy than equation (24). In order to use the above representation of the 2nd- order difference operator, one needs to multiply the FD equation through out by the denominator and then rearrange terms to solve for the unknown.

Implicit finite-difference formula for the 1st-order derivatives

Motivated by Formula (26), an implicit finite-difference formula for the first-order derivatives can be expressed as (Liu and Sen, 2009a)

$$\frac{\partial p}{\partial x} \approx \frac{\dfrac{1}{h}\sum_{n=-N}^{N} c_n p(x+nh)}{1+bh^2\dfrac{\delta^2}{\delta x^2}}, \qquad \text{……….(27).}$$

where, the difference operator in the denominator is a 2nd-order centered finite difference stencil, c_n, an odd discrete sequence, and b can be computed by solving the following equations (Liu and Sen, 2009a)

$$\begin{bmatrix} 1^0 & 2^0 & \cdots & N^0 & 0 \\ 1^2 & 2^2 & \cdots & N^2 & -3 \\ 1^4 & 2^4 & \cdots & N^4 & -5 \\ \vdots & \vdots & \cdots & \vdots & \vdots \\ 1^{2N} & 2^{2N} & \cdots & N^{2N} & -(2N+1) \end{bmatrix} \begin{bmatrix} 1c_1 \\ 2c_2 \\ \vdots \\ Nc_N \\ b \end{bmatrix} = \begin{bmatrix} 1/2 \\ 0 \\ 0 \\ \vdots \\ 0 \end{bmatrix}. \qquad \text{…....(28)}$$

Implicit finite-difference formula for the 2nd-order derivatives

An implicit finite-difference formula for the second-order derivatives can be expressed as (Liu and Sen, 2009a)

$$\frac{\partial^2 p}{\partial x^2} \approx \frac{\dfrac{1}{h}\sum_{n=-N}^{N} c_n p(x+nh)}{1+bh^2\dfrac{\delta^2}{\delta x^2}}, \qquad \text{………. (29).}$$

where, c_n is an even discrete sequence, $c_0 = -2\sum_{n=1}^{N} c_n$, $c_n (n=1,2,\cdots,N)$ and b can be computed by solving the following equations (Liu and Sen, 2009a)

$$\begin{bmatrix} 1^0 & 2^0 & \cdots & N^0 & 0 \\ 1^2 & 2^2 & \cdots & N^2 & -3\times 4 \\ 1^4 & 2^4 & \cdots & N^4 & -5\times 6 \\ \vdots & \vdots & \cdots & \vdots & \vdots \\ 1^{2N} & 2^{2N} & \cdots & N^{2N} & -(2N+1)(2N+2) \end{bmatrix} \begin{bmatrix} 1^2 c_1 \\ 2^2 c_2 \\ \vdots \\ N^2 c_N \\ b \end{bmatrix} = \begin{bmatrix} 1 \\ 0 \\ 0 \\ \vdots \\ 0 \end{bmatrix}.$$

……….. (30)

The following expressions are respectively used to examine the accuracy of implicit finite-difference formulas (27) and (29) (Liu and Sen, 2009a)

$$g_1(\alpha) = \frac{\sum_{n=1}^{N} c_n \sin(2n\alpha)}{1-4b\sin^2\alpha}, \qquad \text{………. (31a)}$$

$$g_2(\alpha) = \sqrt{\frac{-\frac{1}{4}c_0 - \frac{1}{2}\sum_{n=1}^{N} c_n \cos(2n\alpha)}{1-4b\sin^2\alpha}}. \qquad \text{………. (31b)}$$

The exact values of the above expressions are α, and the calculated values are compared with α for different order numbers determined by *N*, shown in Figure 6. We can see that the accuracy increases with the increase of the order number. Comparing Figure 5 with Figure 6, we note that for the same order number, the accuracy of the implicit method is better than that of the corresponding explicit method. It has been found (Liu and Sen, 2009a) that for standard-grid finite differences, the accuracy of a (2*N*+2)th-order implicit formula (27) is nearly equivalent to that of a (6*N*+2)th-order explicit formula (17) for the first-order derivative, and a (2*N*+2)th-order implicit formula (29) is nearly equivalent to a (4*N*+2)th-order explicit formula (20) for the second-order derivative. Because the computation cost of a (2*N*+2)th-order IFDM is equal to that of an EFDM of some order plus that of solving tridiagonal equations, a high-order EFDM may be replaced by an IFDM of some order, which will increase the accuracy but not the cost of computation.

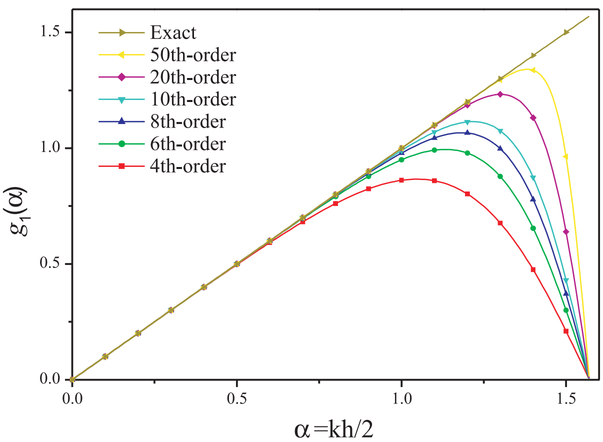

(a) Exact α and $g_1(\alpha)$ of IFDM with different order numbers for the first-order derivative

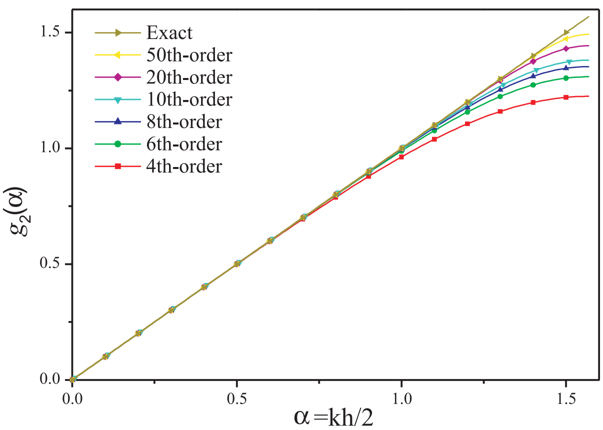

(b) Exact α and $g_2(\alpha)$ of IFDM with different order numbers for the second-order derivative

Fig. 6 Accuracy of implicit finite-difference formulas

Time-space finite-difference methods

In the previous sections, we derived finite-difference stencils of time and space derivatives by using the plane wave theory and the truncated Taylor series in time and space respectively. The finite-difference coefficients are derived independently for time and space derivative operators and the approximations are incorporated into wave equations to arrive at a finite difference based recursion operator. Alternatively, we can apply finite difference approximation of time and space derivatives directly to the wave equations simultaneously and then derive the coefficients.

To demonstrate this, we start with 1D acoustic wave equation in homogenous media given by Equation (1). A 2nd-order finite difference on the time derivatives, given by Equation (2) is usually used. Generally, the modeling accuracy is improved by using a high-order finite difference on the spatial derivatives; a (2*N*)th-order finite-difference formula is given by Equation (5).

Substituting Equations (2) and (5) into Equation (1) and rearranging, we have

$$c_0 p_{j,m} + \sum_{n=1}^{N} c_n \left(p_{j-n,m} + p_{j+n,m}\right) \approx \frac{h^2}{v^2\tau^2}\left[\left(p_{j,m-1} + p_{j,m+1}\right) - 2p_{j,m}\right]. \qquad \text{..........(32)}$$

In the conventional method, the finite-difference coefficients of the space derivatives are determined in the space domain alone and can be determined by Equation (21) to satisfy Equation (5). It can be proved that when we use the (2*N*)th-order space domain finite-difference and the 2nd-order time domain finite-difference stencils to solve the 1D acoustic wave equation, the accuracy order is 2. Obviously, the conclusion is the same for the 2D and 3D acoustic wave equations. It is worthwhile to note that increasing *N* may decrease the magnitude of the finite-difference error but may not increases the accuracy order. The main reason is that the finite-difference stencils are designed in the space and time domains separately, but the wave equation must be solved in both the space and time domains simultaneously.

To address this issue, i.e., not to satisfy Equation (5) but to satisfy Equation (32), a unified methodology (Finkelstein and Kastner, 2007) has been proposed to derive the finite-difference coefficients in the joint time-space domain. The key idea of this method is that the dispersion relation is completely satisfied at some designated frequencies. Thus several equations are formed and the finite-difference coefficients are obtained by solving these equations simultaneously. It is obvious that there is no dispersion at these designated frequencies when these coefficients are used in modeling. However, since different specific frequencies give different results and dispersion at other frequencies is not easily controlled, this method may not be very useful in practice.

Liu and Sen (2009b) developed a new method similar to Finkelstein and Kastner (2007) which employs a plane wave theory and the Taylor series expansion of dispersion relation to derive the finite-difference coefficients in the joint time-space domain for acoustic wave equation. Using the approach of Liu and Sen (2009b), the following finite-difference coefficients are obtained

$$c_n = \begin{cases} \dfrac{(-1)^{n+1}}{n^2} \prod\limits_{1\le m\le N,\, m\ne n} \left| \dfrac{m^2 - r^2}{m^2 - n^2} \right| & (n = 1, 2, \ldots, N) \\ 2\sum\limits_{m=1}^{N} c_m & (n = 0), \end{cases} \qquad \text{..........(33)}$$

where, $r = v\tau/h$. When $r = 0$, the finite-difference coefficients are the same as Equation (21). That is, the conventional method is just a special case of the new method. The 1D finite-difference modeling method by using these new coefficients from Equation (33) can reach (2N)th-order accuracy.

A parameter δ is defined as follows to describe the dispersion of 1D finite-difference modeling

$$\delta = \frac{v_{FD}}{v} = \frac{2}{rkh} \sin^{-1} \sqrt{r^2 \sum_{n=1}^{N} c_n \sin^2(nkh/2)}. \qquad \text{..........(34)}$$

If δ equals 1, there is no dispersion. If δ is far from 1, a large dispersion will occur. Because kh is equal to π at the Nyquist frequency, kh only ranges from 0 to π when calculating δ.

Figure 7 shows the variation of the dispersion parameter δ with kh for different space point numbers. The involved parameters are listed in the figure. This figure demonstrates that

- ❖ Dispersion decreases with the increase of N.
- ❖ For the conventional method, δ nearly equals 1 when $kh < 0.6$. The area where δ nearly equals 1 does not extend with the increase of N. That is, increasing N decreases the magnitude of the dispersion error but does not increase the accuracy order.
- ❖ For the new method, the area where δ nearly equals 1 obviously extends with the increase of N.
- ❖ The accuracy of the new method is greater than that of the conventional method.

As an example, the initial conditions of Equations

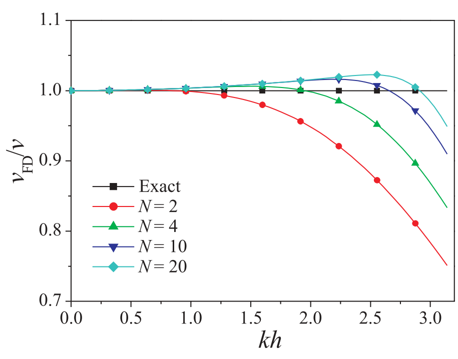

(a) Conventional method

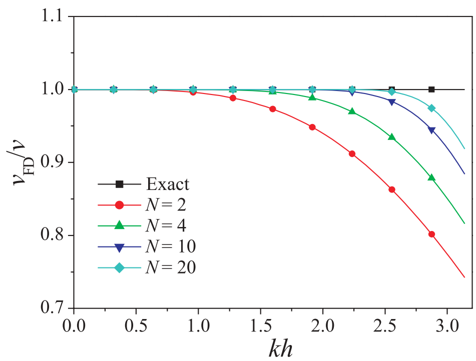

(b) New method

Fig. 7 1D dispersion curves of the conventional and new methods for different space point numbers 2N+1, N = 2, 4, 10, 20, v = 3000m/s, τ = 0.001s, h = 10m.

12(a) and 12(b) are used to perform modeling. Figure 8 shows the records for different velocities. The dispersion of the new method with finite-difference coefficients determined by Equation (33) is smaller than that of the conventional method finite-difference coefficients determined by Equation (5). The variation of the velocity affects the results of the conventional method more than the new method because the finite-difference coefficients of the new method depend on velocity.

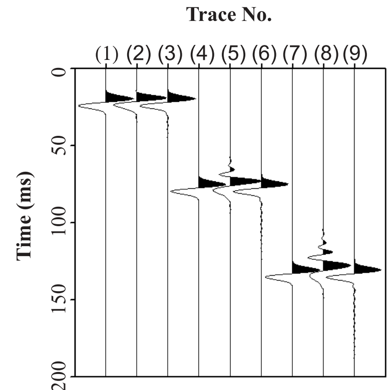

(a) v = 4500m/s

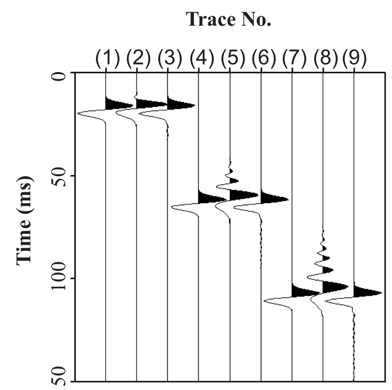

(b) v = 5500m/s

Fig. 8 1D modeling records by conventional EFDM and new time-space domain EFDM for different velocities. (1), (4) and (7) are analytic solutions; (2), (5) and (8) are modeling results from the conventional method, (3), (6) and (9) are modeling results from the new method. Distances between source center and these three receivers are 100m, 350m and 600m respectively. α^2 = 2, h = 10m, τ = 0.001s, N = 20.

This new time-space domain method has been extended to solve 2D acoustic wave equation and can reach (2N)th-order accuracy along 8 directions (Liu and Sen, 2009c).

Numerical modeling examples

To demonstrate the effects of different finite-difference methods stated in this paper, we perform numerical modeling of 2D acoustic wave equation for the SEG/EAGE salt model using the following 2D acoustic wave equation

$$\frac{\partial^2 p}{\partial x^2}+\frac{\partial^2 p}{\partial z^2}=\frac{1}{v^2}\frac{\partial^2 p}{\partial t^2}. \quad \ldots\ldots\ldots(35)$$

In the modeling algorithm, temporal derivatives are discretized by second-order finite difference similar to Equation (2). Spatial derivatives are discretized by following three finite-difference methods discussed earlier. The first method is a conventional 14th-order EFDM; its discretization formula is given in Equation (20) and the finite-difference coefficients are determined by Equations (21). The second one is a 14th-order IFDM; its discretization formula is given in Equation (29) and the coefficients are determined by Equations (30). The third one is a 28th-order time-space domain FDM; its discretization formula is given in Equation (20) and the coefficients are determined in the joint time-space domain (Liu and Sen, 2009c). It has been reported that the 14th-order IFDM is nearly equivalent to the conventional 28th-order EFDM (Liu and Sen, 2009a).

The SEG/EAGE salt model is shown in Figure 9(a); some modeling parameters are given in the caption of Figure 9. Here, we simply extend the model spatially to avoid reflections from the top and other edges of the model. The modeling snapshots are shown in Figures 9(b), 9(c) and 9(d). The modeling records are shown in Figures 9(e), 9(f) and 9(g). Partially enlarged views of these three figures are shown in Figures 9(h), 9(i) and 9(j). Comparing these modeling results, we can see that the accuracy of the 14th-order IFDM is greater than that of the conventional 14th EFDM. The 28th-order time-space domain FDM can retain the waveform better than the conventional 28th-order EFDM or the 14th-order IFDM.

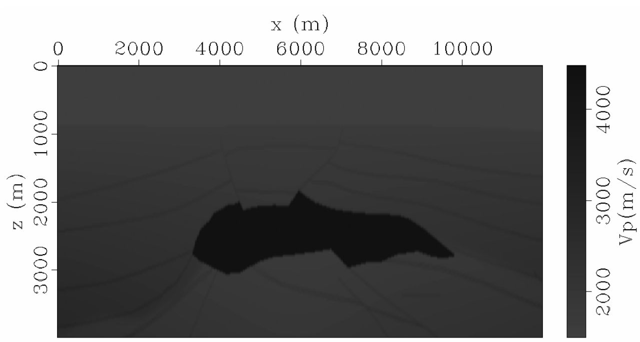

(a) SEG/EAGE salt model

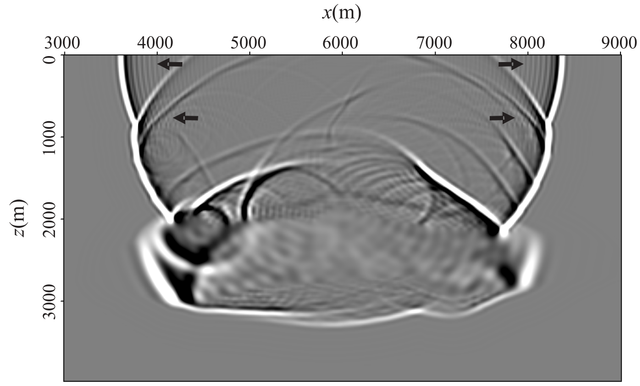

(b) Snapshot computed by the conventional 14th-order EFDM

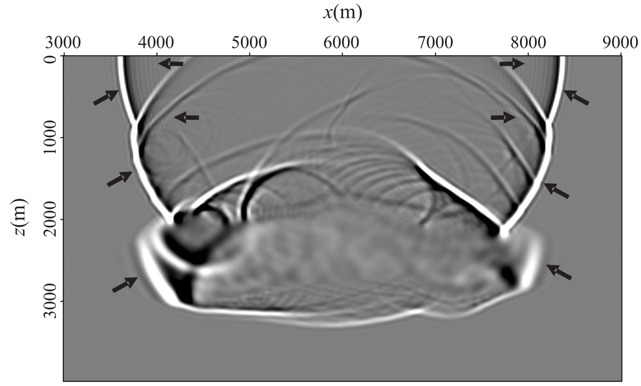

(c) Snapshot computed by the 14th-order IFDM (equivalent to the conventional 28th-order EFDM)

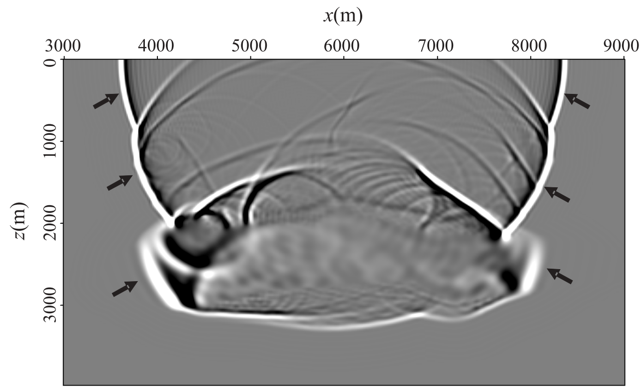

(d) Snapshot computed by the 28th-order time-space domain FDM

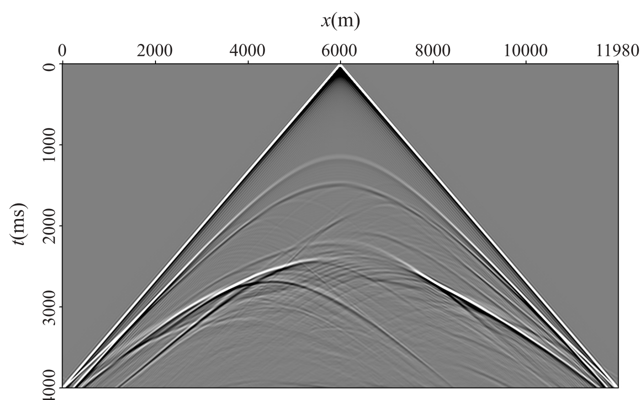

(e) Seismograms by the conventional 14th-order EFDM

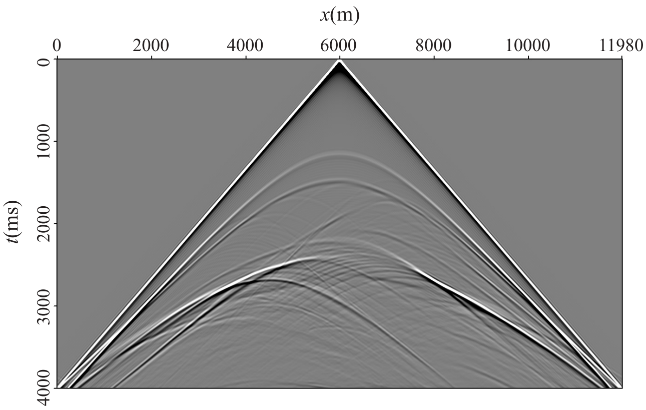

(f) Seismograms computed by the 14th-order IFDM (equivalent to the conventional 28th-order EFDM)

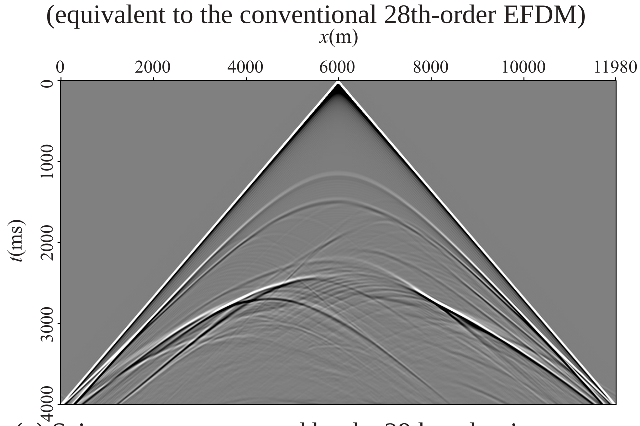

(g) Seismograms computed by the 28th-order time-space domain FDM

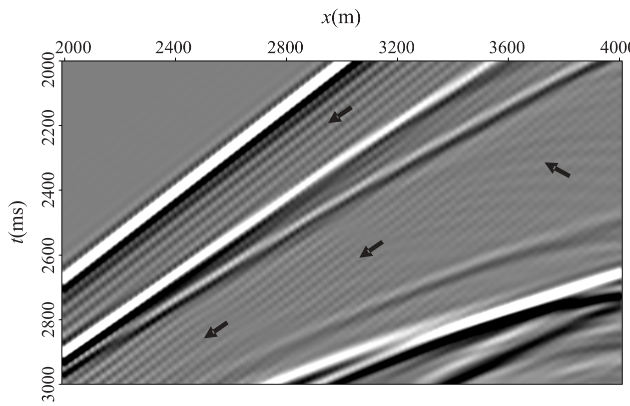

(h) Zoom of (e)

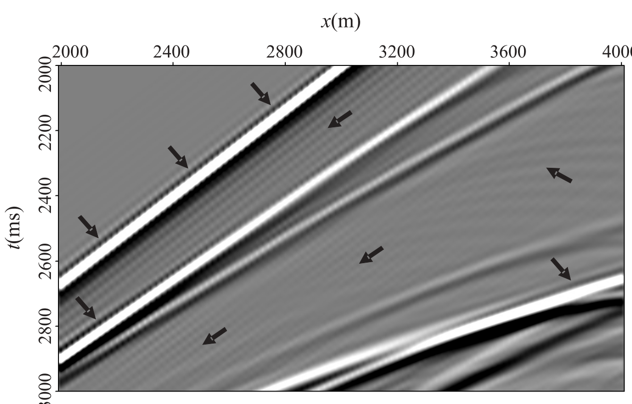

(i) Zoom of (f)

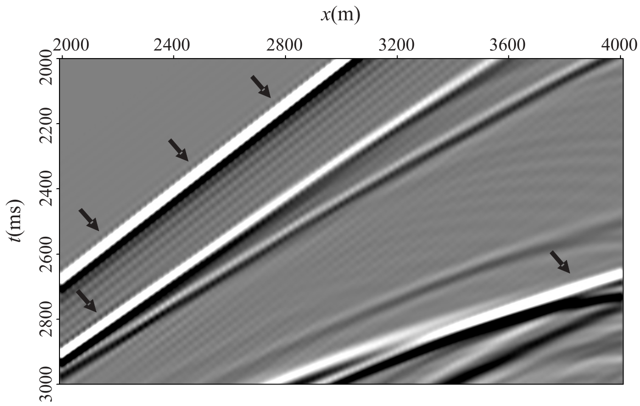

(j) Zoom of (g)

Fig.9 Numerical modeling results of 2D acoustic wave equation for the SEG/EAGE salt model by the conventional 14th EFDM, the 14th-order IFDM (equivalent to conventional 28th-order EFDM) and the 28th-order time-space domain FDM. τ = 0.002s, h = 20m. The coordinate of the source is (6000m, 20m). A one-period sine function with 20Hz frequency is used as the source wavelet. Time of snapshots is 1600ms.

Conclusions

The finite difference methods for seismic wavefield modeling and imaging are considered to be the most accurate since these methods are capable of computing all the wave modes. In addition there is no restriction on the complexity of a geologic model as long as we can represent the model in a discrete form. However, these methods indeed suffer from numerical inaccuracy resulting from approximating a derivative operator and discretization of a geologic model. Novel finite-difference operators can be derived to address this issue. In this paper, we have reviewed the developments of arbitrary even-order FDMs with application to acoustic wave equation. The accuracy of these methods increases with the increase of order number. Since the accuracy is determined by the order number and grid size, arbitrary even-order FDMs can provide a trade-off between the order number and grid size for a given accuracy. The IFDMs require solving tridiagonal matrix equations only. Some high-order EFDM may be replaced by an IFDM of some order to decrease the computation time and retain the accuracy. High-order spatial FD stencils designed in the joint time-space domain can improve the accuracy further for acoustic wave equation modeling. This time-space domain method can be extended to solve not only the acoustic wave equation but also other similar partial difference equations.

Acknowledgements

Liu would like to thank China Scholarship Council for their financial support for this research and UTIG for providing with the facilities. This research is also partially supported by NSFC under contract No. 40839901 and the National “863” Program of China under contract No. 2007AA06Z218.

References

Bansal, R., and M. K. Sen, 2008, Finite-difference modelling of S-wave splitting in anisotropic media: Geophysical Prospecting, 56, 293-312.

Bohlen, T., and E. H. Saenger, 2006, Accuracy of heterogeneous staggered-grid finite-difference modeling of Rayleigh waves: Geophysics, 71, T109–T115.

Chen, J., 2007, High-order time discretizations in seismic modeling: Geophysics, 72, SM115–SM122.

Chen J. F., and Guan Z., 1989, Numerical solution of partial differential equations, Tsinghua University Press, Beijing, China

Claerbout, J. F., 1985, Imaging the earth's interior: Blackwell Scientific Publications, Inc., Palo. Alto, CA, USA

Crase E., 1990, High-order (space and time) finite-difference modeling of the elastic wave equation: 60th Annual International Meeting, SEG, Expanded Abstracts, 987-991.

Dablain, M. A., 1986, The application of high-order differencing to the scalar wave equation: Geophysics, 51, 54–66.

Dong L. G., Z T Ma, et. al., 2000, A staggered-grid high-order difference method of one-order elastic wave equation: Chinese Journal of Geophysics, 43: 411-419.

Emerman, S., W. Schmidt, and R. Stephen, 1982, An implicit finite-difference formulation. of the elastic wave equation: Geophysics, 47, 1521-1526.

Etgen, J. T., and M. J. O'Brien, 2007, Computational methods for large-scale 3D acoustic finite-difference modeling: A tutorial: Geophysics, 72, SM223–SM230.

Fei, T., and C. L. Liner, 2008, Hybrid fourier finite difference 3D depth migration for anisotropic media: Geophysics, 73, S27-S34.

Fornberg, B., 1987, The pseudospectral method - comparisons with finite differences for the elastic wave equation: Geophysics, 52, 483-501.

Gold, N., S. A. Shapiro, and E. Burr, 1997, Modeling of high contrasts in elastic media using a modified finite difference scheme: 68th Annual International Meeting, SEG, Expanded Abstracts, ST 14.6.

Finkelstein, B., and R. Kastner, 2007, Finite difference time domain dispersion reduction schemes: Journal of Computational Physics, 221, 422–438.

Graves, R., 1996, Simulating seismic wave propagation in 3D elastic media using staggered-grid finite differences: Bulletin of the Seismological Society of America, 86, 1091–1106.

Hayashi, K., and D. R. Burns, 1999, Variable grid finite-difference modeling including surface topography: 69th Annual International Meeting, SEG, Expanded Abstracts, 523-527.

Igel, H., P. Mora, and B. Riollet, 1995, Anistotropic wave propagation through finite-difference grids: Geophysics, 60, 1203–1216.

Kelly, K. R., R. Ward, W. S. Treitel, and R. M. Alford, 1976, Synthetic seismograms: A finite-difference approach: Geophysics, 41, 2–27.

Kindelan M., A. Kamel, and P. Sguazzero, 1990, On the construction and efficiency of staggered numerical differentiators for the wave equation: Geophysics, 55, 107-110.

Lele, S. K., 1992, Compact finite difference schemes with spectral-like resolution, Journal of Computational Physics, 103, 16–42

Levander, A., 1988, Fourth-order finite-difference P-SV seismograms: Geophysics, 53, 1425–1436.

Li, Z., 1991, Compensating finite-difference errors in 3-D migration and modeling: Geophysics, 56, 1650-1660.

Liu, Y., C. Li, and Y. Mou, 1998, Finite-difference numerical modeling of any even-order accuracy: Oil Geophysical Prospecting (Abstract in English), 33, 1-10.

Liu, Y., and X. Wei, 2008, Finite-difference numerical modeling with even-order accuracy in two-phase anisotropic media: Applied Geophysics, 5, 107-114.

Liu Y., and M. K. Sen, 2009a, A practical implicit finite-difference method: examples from seismic modeling: Journal of Geophysics and Engineering, 6, 231-249.

Liu Y., and M. K. Sen, 2009b, A new time-space domain high-order finite-difference method for acoustic wave equation, CPS/SEG Beijing 2009 International Geophysical Conference, Expanded abstract, ID54

Liu Y., and M. K. Sen, 2009c, 2D acoustic wave equation modeling with a new high-accuracy time-space domain finite-difference stencil, 71st EAGE Conference, Extended Abstracts, S011

Opršal, I., and J. Zahradník, 1999, Elastic finite-difference method for irregular grids: Geophysics, 64, 240–250.

Pei Z., 2004, Numerical modeling using staggered-grid high order finite-difference of elastic wave equation on arbitrary relief surface: Oil Geophysical Prospecting (Abstract in English), 39, 629-634.

Robertsson, J., J. Blanch, and W. Symes, 1994, Viscoelastic finite-difference modeling: Geophysics, 59, 1444–1456.

Saenger, E., and T. Bohlen, 2004, Finite-difference modeling of viscoelastic and anisotropic wave propagation using the rotated staggered grid: Geophysics, 69, 583–591.

Tessmer, E., 2000, Seismic finite-difference modeling with spatially varying time steps: Geophysics, 65, 1290-1293.

Virieux, J., 1986, P-SV wave propagation in heterogeneous media: Velocity stress finite difference method: Geophysics, 51, 889–901.

Wang, Y. and G. T. Schuster, 1996, Finite-difference variable grid scheme for acoustic and elastic wave equation modeling: 66th Annual International Meeting, SEG, Expanded Abstracts, 674-677.

Zhang, G., Y. Zhang, and H. Zhou, 2000, Helical finite-difference schemes for 3-D. depth migration: 69th Annual International Meeting, SEG, Expanded Abstracts, 862–865.

Zhang, H., and Y. Zhang, 2007, Implicit Splitting Finite Difference Scheme for Multi-dimensional Wave Simulation: 75th Annual International Meeting, SEG, Expanded Abstracts, 2011-2014.

Appendix A : Derivation of Equation (14)

Equation (7) can be rewritten as follows

$$p_{j,m+1} = \left(2 + r^2 c_0\right) p_{j,m} + r^2 \sum_{n=1}^{N} c_n \left(p_{j-n,m} + p_{j+n,m}\right) - p_{j,m-1}. \quad \text{(A1)}$$

Substituting Equation (13) into (A1) and simplifying it, we have

$$p_{j,m+1} = \left[\left(2 + r^2 c_0\right) + r^2 \sum_{n=1}^{N} c_n 2\cos(nkh)\right] w_{1,m} e^{ijkh} - w_{2,m} e^{ijkh}. \quad \text{(A2)}$$

Equation (13) gives

$$q_{j,m+1} = p_{j,m} = w_{1,m} e^{ijkh}. \quad \text{(A3)}$$

Write (A2) and (A3) as matrix form

$$\begin{bmatrix} p_{j,m+1} \\ q_{j,m+1} \end{bmatrix} = \begin{bmatrix} \left(2 + r^2 c_0\right) + r^2 \sum_{n=1}^{N} c_n 2\cos(nkh) & -1 \\ 1 & 0 \end{bmatrix} \boldsymbol{W}_m e^{ijkh}. \quad \text{(A4)}$$

Equation (13) also gives

$$\begin{bmatrix} p_{j,m+1} \\ q_{j,m+1} \end{bmatrix} = \boldsymbol{W}_{m+1} e^{ijkh}. \quad \text{(A5)}$$

Finite-difference coefficients for 2nd-order derivative satisfy

$$c_0 = -2 \sum_{n=1}^{N} c_n. \quad \text{(A6)}$$

Substituting Equations (A5) and (A6) into (A4) and simplifying it, we obtain

$$\boldsymbol{W}_{m+1} = \begin{bmatrix} 2 + 2r^2 \sum_{n=1}^{N} c_n \left(\cos(nkh) - 1\right) & -1 \\ 1 & 0 \end{bmatrix} \boldsymbol{W}_m. \quad \text{(A7)}$$

Appendix B : A methodology based on plane wave theory for deriving finite-difference coefficients

Finite-difference coefficients are determined by satisfying finite-difference formulas, such as Equations (17), (20), (27), (29) and (32). We give a methodology based on plane wave theory for deriving finite-difference coefficients with an example for Equation (17). The methodology includes 5 steps. First, according to a plane wave theory, we express the wave field as

$$p(x + nh) = e^{ik(x+nh)}.$$

Second, substitute this function into finite-difference formula and simplify it, this results in

$$k \approx \frac{2}{h} \sum_{n=1}^{N} c_n \sin(nkh).$$

Third, use the Taylor series expansion for trigonometric function,

$$kh \approx 2 \sum_{n=1}^{N} c_n \left(\sum_{m=1}^{\infty} (-1)^{m-1} \frac{(nkh)^{2m-1}}{(2m-1)!} \right).$$

Fourth, compare the coefficients and obtain several equations,

$$\frac{2(-1)^{m-1}}{(2m-1)!} \sum_{n=1}^{N} n^{2m-1} c_n = \begin{cases} 1 & (m = 1) \\ 0 & (m = 2,3,\ldots,N) \end{cases}.$$

Finally, solve these equations to obtain finite-difference coefficients .

The detailed derivations of finite-difference coefficients for Equations (17), (20), (27), (29) and (32) can be found in some papers (Liu and Sen, 2009a, 2009b, 2009c).